Solitary waves in diatomic chains

Anna Vainchtein, Yuli Starosvetsky, J. Douglas Wright, and Ron Perline

Phys. Rev. E **93**, 042210 — Published 18 April 2016

DOI: 10.1103/PhysRevE.93.042210

Solitary waves in diatomic chains

Anna Vainchtein,[1] Yuli Starosvetsky,[2] J. Douglas Wright,[3] and Ron Perline[3]

[1]*Department of Mathematics, University of Pittsburgh, Pittsburgh, Pennsylvania 15260, USA,* aav4@pitt.edu

[2]*Faculty of Mechanical Engineering, Technion Israel Institute of Technology, Technion City, Haifa 3200, Israel*

[3]*Department of Mathematics, Drexel University, Philadelphia, PA 19104*

We consider the mechanism of formation of isolated localized wave structures in the diatomic Fermi-Pasta-Ulam (FPU) model. Using a singular multiscale asymptotic analysis in the limit of high mass mismatch between the alternating elements, we obtain the typical slow-fast time scale separation and formulate the Fredholm orthogonality condition approximating a sequence of mass ratios supporting the formation of solitary waves in the general type of diatomic FPU models. This condition is made explicit in the case of diatomic Toda lattice. Results of numerical integration of the full diatomic Toda lattice equations confirm the formation of these genuinely localized wave structures at special values of the mass ratio that are close to the analytical predictions when the ratio is sufficiently small.

PACS numbers: 05.45.Yv,45.50.-j,46.40.Cd

I. INTRODUCTION

Over the last several decades formation of localized excitations in dynamical systems has drawn a considerable interest because solutions of this type describe some fundamental mechanisms that emerge in many physical settings, including electrical networks, nonlinear optics, ion acoustic waves in plasma, dislocations in crystals, dynamics of polymer chains, granular metamaterials and more [1–3]. Seminal works by Fermi, Pasta and Ulam [4] and Zabusky and Kruskal [5] have initiated the extensive studies of dynamics of monatomic nonlinear lattices and the related soliton-like excitations. In particular, the fundamental problem of the formation of localized excitations (solitary waves, traveling breathers) in the Fermi-Pasta-Ulam (FPU) models induced by a local initial perturbation has become one of the broadly studied topics in dynamics of nonlinear lattices [6]. It is well known that in many cases presence of nonlinearity in the FPU models can balance the dispersive effects and support the formation of coherent localized structures such as solitary waves propagating with a constant amplitude-dependent speed. Existence of solitary waves in a general class of homogeneous FPU models was proven by Friesecke and Wattis [7]. It was also shown that long-wave and short-wave approximations of the infinite FPU chain result in the well known nonlinear integrable partial differential equations, namely, Korteweg de Vries (KdV) and nonlinear Schrödinger (NLS) equations, respectively, that have dynamical solitons (KdV) and envelope solitons (NLS) as their particular solutions [2].

Other fundamental problems of solitary wave excitations in nonlinear lattices concerned periodically heterogeneous diatomic and polyatomic FPU models. These problems have naturally emerged due to their important applications in physics and mechanics. Models of diatomic lattices have been used as prototypes to approach the transport of energy [8] and describe the dynamics of materials (such as ferroelectric perovskites) that present a quasi-1D diatomic structure along certain crystallographic directions [9]. For complicated polyatomic systems like molecular-hydrogen-bonded chains [10, 11], the problem becomes tractable by selecting the most important degrees of freedom and using a diatomic model. Propagation of solitary waves along diatomic chains was analyzed in [12] and [13], where second-neighbor interactions were also included. Using a quasicontinuum approximation, the authors obtained different solutions for soliton-like excitations, including subsonic and supersonic acoustic kinks and optical envelope solitons. Rigorous approximation results along these lines were established in [14–16]. Quasicontinuum approximations were also used to analyze solitary-like excitations and traveling kinks in diatomic lattices in [17–20]. Numerical simulations of these systems reveal the existence of small oscillatory tails in the wake of these solitary-like

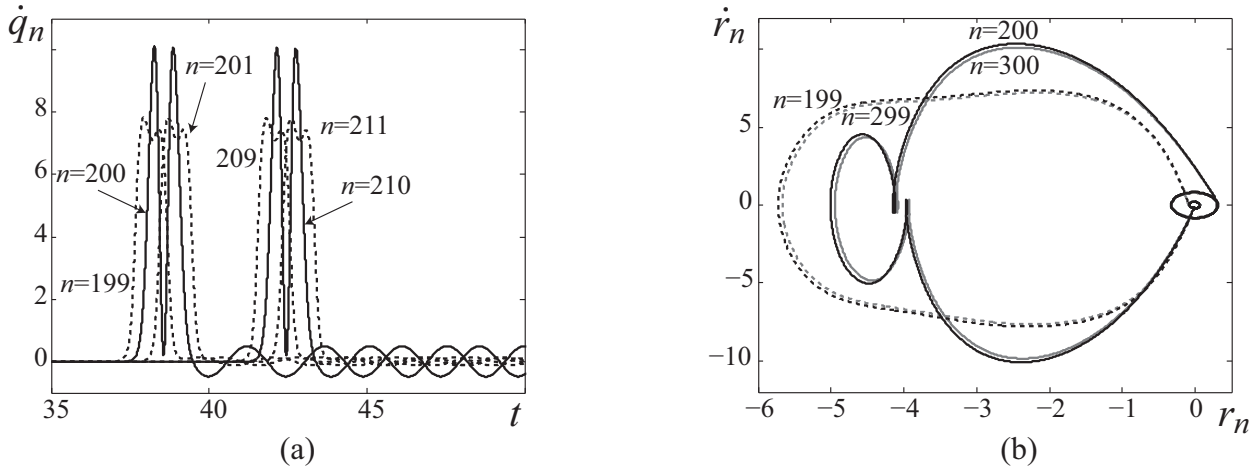

FIG. 1. (a) Velocity profiles $\dot{q}_n(t)$ for light (solid curves) and heavy (dotted curves) masses at $n = 199$, 200, 201 and $n = 209$, 210, 211 solving (5) with $\phi'(r) = 1 - e^{-r}$. The amplitude of emitted oscillations is larger for the light masses. (b) A 'phase plane' plot of relative velocity $\dot{r}_n = \dot{q}_{n+2} - \dot{q}_n$ between the neighboring heavy (odd n) or light (even n) masses versus the relative displacement $r_n = q_{n+2} - q_n$ at $n = 199$ (dashed black curve), $n = 200$ (solid black), $n = 299$ (dashed gray), $n = 300$ (solid gray). Here the mass ratio is $\varepsilon = 0.35$, and the initial condition is determined from (19), (20) with $\kappa = \mathrm{arcsinh}(2\sqrt{5})$.

pulses which are sometimes referred to as long-lived quasi-solitons. Waves radiated by a propagating solitary pulse and propagating behind it are known to be a *generic* feature of diatomic (and, more generally, polyatomic) systems and are associated with the *optical* dispersion branches present in such settings. They reduce the energy and amplitude of the propagating pulse, resulting in its permanent distortion [21–24]. This is illustrated in Fig. 1 showing pulse-like solutions in the diatomic Toda lattice, where one can clearly see two distinct pulses propagating through the heavy (odd-numbered) and light (even-numbered) masses. The pulses emit oscillations in their wake and slightly decrease in amplitude as they move through the lattice. Emergence of the optical vibrations in the diatomic problem is not surprising, given that the corresponding optical linear spectrum is present in the supersonic regime, which in the monatomic case is associated with formation of genuine solitary waves due to the absence of resonances with the acoustic spectrum. One of the most interesting questions which naturally arises in this context is whether there exist some special localized solutions in the polyatomic discrete media that are *isolated*, i.e. exist for some particular choice of the system parameters, and propagate with no energy radiation to the far field.

Following the groundbreaking discovery by Fujioka and Espinosa [25], formation of the brand-new category of isolated localized solutions (solitary waves) in dispersive nonlinear media has become a subject of the intense research [26–30]. As shown in these works, this special class of solitary

waves can exist under conditions which prior to [25] were thought to be impossible. In particular, it was believed that for a soliton to exist, it is absolutely necessary that no resonance occurs between the soliton and these linear waves. Otherwise, energy will be radiated from the core of the solitary pulse through the phononic modes. However, as these studies have shown, isolated solitary waves, called *embedded solitons*, whose wave number is contained ("embedded") in the linear spectrum of the system can exist in several variants of NLS models [25–30]. These special solitary wave solutions are isolated, i.e. associated with discrete sets of unique amplitudes and wave numbers that are defined by the system parameters, and appear to be semistable. However, additional studies of the embedded soliton solutions in various continuous physical models (e.g. the interaction of three spatial solitons propagating in a planar waveguide with a quadratic nonlinearity [31, 32], modified KdV [33], extended KdV [34]) have indicated that these waves can exist in continuous families and be stable. Further studies of the embedded solitons have also shown their existence in the discrete models [35]. Rigorous analysis of these solutions in various systems can be found in [36–38]. In a recent work [39] authors have analyzed a general class of dispersive nonlinear systems and formulated sufficient conditions for the existence of a countable infinity of single humped, embedded solitons. In the same study an approximate infinite sequence of the system parameter values corresponding to these unique isolated solutions has been found using asymptotic methods.

In the context of polyatomic FPU models, existence of genuine stable solitary wave solutions that have no oscillatory tail has also been of considerable interest. First numerical observation of such wave emerging in the diatomic FPU lattice for a certain mass ratio was reported in [23]. In this work the author has considered numerically the response of the diatomic Toda lattice subjected to the initial perturbation in the form of the solitary wave of the underlying homogeneous Toda chain [40]. Formation of a localized wave pulse propagating along the periodic (diatomic) lattice with negligible distortion has been observed for some particular ratio of the heavy and the light masses in the chain. Another numerical study of solitary wave propagation in nonhomogeneous Toda lattice with periodic and aperiodic structure reported the formation of "nearly" genuine stable solitary waves [21]. This observation of the localized wave existing in the diatomic Toda lattice has motivated the work [41], where the formation of the discrete set of such pulses excited in heterogeneous Toda chain has been analytically predicted for the hard-core limit. As reported in [24, 42], an infinite set of these localized wave structures can also be realized in various configurations of highly nonlinear and non-smooth polyatomic discrete system such as diatomic granular crystals [43, 44]. The authors of [24, 42] show that formation of these waves is governed by a peculiar mechanism of anti-resonance established between the phase of the fast oscillations of the light masses and the phase of the

primary pulse transmission.

Motivated by these results, we analyze the intrinsic mechanism of formation of solitary waves in a general class of diatomic FPU models. We perform singular multiscale asymptotic analysis in the limit of high mass mismatch between the alternating elements. In this limit there exists a separation between slow and fast time scales. The slow time scale is associated with the propagation of the primary pulse through the heavy elements while the fast time scale describes the oscillations of the light elements inertially excited by the heavy ones. This fast dynamics of the light masses is captured by a single oscillator that has a slowly varying natural frequency and is driven by an external excitation induced by the solitary wave transmission through the heavy elements. Using the associated asymptotic equation, we formulate the anti-resonance Fredholm orthogonality condition that approximates the special mass ratio values supporting the formation of solitary waves. To showcase the validity of the formulated analytical prediction we then consider the diatomic Toda lattice in the limit of high mass mismatch. Importantly, in contrast to the previously considered case of granular crystals [24, 42], the diatomic Toda lattice setting enables us to find exact solutions of the derived singular asymptotic equations. In particular, the Fredholm condition reduces to orthogonality of an explicit odd solution of time-independent Schrödinger equation with a Pöschl-Teller potential and an odd function derived from the exact solution of the monatomic Toda lattice, yielding special mass ratios as zeroes of a certain function that can be directly evaluated. Using known asymptotics of the solutions of the Schrödinger equation, we also obtain a simplified condition that provides an excellent approximation of the anti-resonance values in a certain parameter regime. The obtained analytical predictions are supported by numerical simulations of the full diatomic Toda lattice, which suggest existence of genuine solitary waves at certain mass ratios. When the mass ratios are sufficiently small, the numerically obtained anti-resonance values are close to the analytical predictions.

The structure of the paper is as follows. Section II is devoted to the general problem statement. In Section III we perform the singular multiscale analysis and formulate the Fredholm orthogonality condition for mass ratios associated with formation of isolated solitary waves in the general class of FPU chains. In Section IV we show that in the case of the diatomic Toda lattice these waves are formed when an integral involving two explicitly known functions vanishes. Derivation of the exact formula for this integral evaluated at a certain sequence of mass ratios is presented in the Appendix. A simplified anti-resonance condition is derived in Section V. Simulation results for the full diatomic Toda lattice and verification of the obtained asymptotic predictions are presented in Section VI. We conclude with Section VII highlighting the most important findings of this work

along with their potential extensions and open problems.

II. PROBLEM FORMULATION

Consider an infinite one-dimensional diatomic lattice with energy given by the Hamiltonian

$$\mathcal{H} = \sum_{n=-\infty}^{\infty} \phi(q_n - q_{n-1}) + \frac{1}{2} m_n \dot{q}_n^2.$$

Here m_n is the mass of nth particle, which alternates between $m_{2p-1} = m_1$ and $m_{2p} = m_2 \leq m_1$, $q_n(t)$ is the displacement of nth particle at time t with derivative $\dot{q}_n$, and $\phi(r)$ is the interaction potential. The dynamics of the system is governed by

$$m_n \ddot{q}_n = \phi'(q_{n+1} - q_n) - \phi'(q_n - q_{n-1}). \tag{1}$$

We assume that

$$\phi \in C^2, \quad \phi(0) = \phi'(0) = 0, \quad \phi''(r) > 0 \tag{2}$$

A specific example we consider in what follows is the Toda interaction potential [40]

$$\phi(r) = \frac{a}{b} e^{-br} + ar - \frac{a}{b}, \tag{3}$$

with $a > 0$, $b > 0$. It is convenient to introduce the dimensionless parameter

$$\varepsilon = m_2/m_1 \tag{4}$$

satisfying $0 < \varepsilon \leq 1$ and rescale the system (1) using the dimensionless variables

$$\bar{t} = t\sqrt{\frac{K}{m_1}}, \quad \bar{q}_n = \frac{q_n}{d}, \quad \bar{\phi} = \frac{\phi}{Kd^2},$$

where d is a relevant length scale and $K = \phi''(0) > 0$. For the Toda lattice, we have $K = ab$ and $d = 1/b$. With the bars on the new variables dropped, this yields the following system:

$$\begin{aligned} \ddot{q}_{2p-1} &= \phi'(q_{2p} - q_{2p-1}) - \phi'(q_{2p-1} - q_{2p-2}) \qquad \text{(heavy masses)} \\ \varepsilon \ddot{q}_{2p} &= \phi'(q_{2p+1} - q_{2p}) - \phi'(q_{2p} - q_{2p-1}) \qquad \text{(light masses).} \end{aligned} \tag{5}$$

With this rescaling the Toda coefficients in (3) are $a = b = 1$, and we have $m_1 = 1$, $m_2 = \varepsilon$.

We are interested in deriving the condition for the existence of solitary wave solutions in the diatomic lattice, i.e. solutions of (5) that have the form

$$q_{2p-1}(t) = u(\xi), \quad q_{2p}(t) = v(\xi), \quad \xi = p - ct, \tag{6}$$

where $c > 0$ is half of the velocity of the wave, with

$$u'(\xi),\ v'(\xi) \to 0 \quad \text{as } |\xi| \to \infty. \tag{7}$$

As mentioned in the Introduction, such solutions do not exist for *generic* values of ε due to the presence of radiative optical oscillations propagating behind the moving pulse and reducing its amplitude and energy (see Fig. 1 for an example). In the following section, we follow the approach in [24] and use multiscale asymptotic analysis at small ε to derive the Fredholm orthogonality condition approximating the special values ε_k at which the oscillatory tails disappear, and the system (5) has solitary wave solutions satisfying (6), (7). We then analyze in Section IV the case of Toda potential, where the approximate existence condition can be made explicit due to the availability of exact solutions of the asymptotic equations.

III. ASYMPTOTIC ANALYSIS

Consider (5) with $0 < \varepsilon \ll 1$. For this high mismatch between the masses, there exists a separation of scales associated with the slow dynamics of the heavy masses governing the propagation of the primary pulse and the inertially excited fast dynamics of the light masses. Following [24], we introduce the fast time $\tau = t/\sqrt{\varepsilon}$ and seek solutions of (5) in the form

$$q_{2p-1} \approx x_{2p-1}(t) + \varepsilon^2 y_{2p-1}(\tau) \quad \text{(heavy masses)},$$
$$q_{2p} \approx x_{2p}(t) + \varepsilon y_{2p}(\tau) \quad \text{(light masses)}.$$

Here the approximation is up to the higher orders of ε. Substituting this in (5), we obtain, up to the higher order terms,

$$\begin{aligned}
\ddot{x}_{2p-1} + \varepsilon y''_{2p-1} &\approx \phi'(x_{2p} - x_{2p-1}) - \phi'(x_{2p-1} - x_{2p-2}) \\
&\quad + \phi''(x_{2p} - x_{2p-1})(\varepsilon y_{2p} - \varepsilon^2 y_{2p-1}) - \phi''(x_{2p-1} - x_{2p-2})(\varepsilon^2 y_{2p-1} - \varepsilon y_{2p-2}) \\
\varepsilon(\ddot{x}_{2p} + y''_{2p}) &\approx \phi'(x_{2p+1} - x_{2p}) - \phi'(x_{2p} - x_{2p-1}) \\
&\quad + \phi''(x_{2p+1} - x_{2p})(\varepsilon^2 y_{2p+1} - \varepsilon y_{2p}) - \phi''(x_{2p} - x_{2p-1})(\varepsilon y_{2p} - \varepsilon^2 y_{2p-1}),
\end{aligned}$$

where $\ddot{x}_n = d^2 x_n/dt^2$ and $y''_n = d^2 y_n/d\tau^2$. The slow $O(1)$ dynamics is then described by

$$\ddot{x}_{2p-1} = \phi'(x_{2p} - x_{2p-1}) - \phi'(x_{2p-1} - x_{2p-2}), \quad x_{2p} = \frac{x_{2p-1} + x_{2p+1}}{2}, \tag{8}$$

where the second equation follows from $\phi'(x_{2p+1} - x_{2p}) = \phi'(x_{2p} - x_{2p-1})$ and the assumed monotonicity of $\phi'(r)$ (recall (2)). Substituting the second equation into the first, one can see that the

slow dynamics of the heavy masses is governed by the equations for the chain of heavy masses only:

$$\ddot{x}_{2p-1} = \phi'\left(\frac{x_{2p+1} - x_{2p-1}}{2}\right) - \phi'\left(\frac{x_{2p-1} - x_{2p-3}}{2}\right), \tag{9}$$

while the dynamics of light masses in slow time is obtained by averaging over the dynamics of the two neighboring heavy masses.

Meanwhile, the fast $O(\varepsilon)$ dynamics is given by

$$\begin{aligned} y''_{2p-1} &= \phi''(x_{2p} - x_{2p-1})y_{2p} + \phi''(x_{2p-1} - x_{2p-2})y_{2p-2} \\ \ddot{x}_{2p} + y''_{2p} &= -\big(\phi''(x_{2p} - x_{2p-1}) + \phi''(x_{2p+1} - x_{2p})\big)y_{2p}. \end{aligned} \tag{10}$$

Observe that the second equation in (10) is decoupled from the first. Moreover, using the second equation in (8) we can rewrite the second equation in (10) for the fast dynamics of the even-numbered light masses in the form

$$y''_{2p}(\tau) + \Omega^2_{2p}(t)y_{2p}(\tau) = f_{2p}(t), \tag{11}$$

which describes uncoupled driven harmonic oscillators with slowly varying natural frequency $\Omega_{2p}(t)$ and driving force $f_{2p}(t)$ given by

$$\Omega^2_{2p}(t) = 2\phi''\left(\frac{x_{2p+1} - x_{2p-1}}{2}\right), \quad f_{2p}(t) = -\ddot{x}_{2p}(t). \tag{12}$$

Assume now that the problem (9) for the slow dynamics of the heavy masses ($\varepsilon = 0$ problem) has a solitary wave solution

$$x_{2p-1}(t) = X(\xi_0), \quad \xi_0 = p - c_0 t, \quad X'(\xi_0) \to 0 \text{ for } |\xi_0| \to \infty. \tag{13}$$

This assumption clearly holds if the monatomic ($\varepsilon = 1$) problem supports solitary waves, existence of which, as proved in [7], is guaranteed for a large class of superquadratic potentials. Then the slow dynamics of light masses is described by $x_{2p}(t) = (X(\xi_0) + X(\xi_0 + 1))/2$, and we have

$$\Omega^2_{2p}(t) = 2\phi''\left(\frac{X(\xi_0 + 1) - X(\xi_0)}{2}\right), \quad f_{2p}(t) = -\frac{c_0^2}{2}\big(X''(\xi_0) + X''(\xi_0 + 1)\big),$$

where we used the second equation in (8) to obtain $f_{2p}(t)$. Since both Ω_{2p} and f_{2p} depend on $t = \tau\sqrt{\varepsilon}$ via ξ_0, the solution of (11) is a function of $\xi_0 = p - c_0\tau\sqrt{\varepsilon}$. It is convenient to rewrite (11) in terms of slow time. It also suffices to consider dynamics of only one oscillator, e.g. the one at $p = 0$, since the rest can be recovered via a time shift. We obtain

$$\ddot{y}_0(t) + \frac{\Omega_0^2(t)}{\varepsilon}y_0(t) = \frac{f_0(t)}{\varepsilon}. \tag{14}$$

Since $X(\xi_0)$ is defined up to an arbitrary translation in its argument, and $X(\xi_0+1)-X(\xi_0)$, $X'(\xi_0+1)+X'(\xi_0)$ have even symmetry about the same point, it is possible to select $X(\xi_0)$ so that $\Omega_0^2(t)$ is even, while $f_0(t)$ is odd. Note also that the behavior of $X(\xi_0)$ in (13) at infinity implies that $f_0(t)\to 0$ and $\Omega_0(t)\to\sqrt{2}$ as $|t|\to\infty$, where we recall that $\phi''(0)=1$ after rescaling. Thus, we expect solutions satisfying $y_0(t)\to 0$ as $t\to-\infty$ to develop oscillations of frequency $\omega=\sqrt{2/\varepsilon}$ at sufficiently large $t>0$ for generic values of ε. We thus seek *special* values at which the amplitude of these oscillations is zero. In other words, we need to find ε such that the corresponding solutions of (14) satisfy the zero conditions at infinity:

$$y_0(t)\to 0 \quad \text{as } |t|\to\infty. \tag{15}$$

Let $Y_1(t;\varepsilon)$ and $Y_2(t;\varepsilon)$ denote two linearly independent solutions of the homogeneous equation $\ddot{y}_0+(\Omega_0^2(t)/\varepsilon)y_0=0$ that are even and odd, respectively, and let α denote their (constant) Wronskian. The method of variation of parameters then yields the following solution of (14) that satisfies $y_0(t)\to 0$ as $t\to-\infty$:

$$y_0(t;\varepsilon)=\frac{1}{\alpha\varepsilon}\left(Y_2(t;\varepsilon)\int_{-\infty}^{t} f_0(s)Y_1(s;\varepsilon)ds - Y_1(t;\varepsilon)\int_{-\infty}^{t} f_0(s)Y_2(s;\varepsilon)ds\right). \tag{16}$$

Since $f_0(t)$ is odd and vanishes at infinity, while $Y_1(t;\varepsilon)$ is even, the first term tends to zero as $t\to\infty$. Meanwhile, at large $t>0$ the equation becomes $\ddot{y}_0+\omega^2 y_0=0$, with $\omega=\sqrt{2/\varepsilon}$, and thus

$$Y_1(t;\varepsilon)\sim A\cos(\omega t+\beta_1), \quad t\to\infty,$$

for some constant $A\neq 0$ and β_1. This yields

$$y_0(t;\varepsilon)\sim -\frac{2A}{\alpha\varepsilon}\cos(\omega t+\beta_1)\int_0^{\infty} f_0(s)Y_2(s;\varepsilon)ds, \quad t\to\infty, \tag{17}$$

where we used the fact that $f_0(t)Y_2(t;\varepsilon)$ is an even function of t. Thus we have oscillations of frequency ω at large $t>0$ *unless*

$$g(\varepsilon)\equiv\int_0^{\infty} f_0(s)Y_2(s;\varepsilon)ds=0. \tag{18}$$

This Fredholm orthogonality condition yields ε such that the solution (16) has no oscillations at infinity, and hence no such waves appear in $q_n(t)$ up to $O(\varepsilon^2)$. Physically, it means that the slow motion of the center of mass of the two neighboring heavy masses, the acceleration of which equals $-f_0(t)$ up to a time shift, does not excite any fast oscillations of the light mass in between at large time. We conjecture that under our assumptions $g(\varepsilon)$ has infinitely many zeroes in the interval $(0,1)$ at $\varepsilon=\varepsilon_k$, $k=1,2,\dots$, with ε_k accumulating at zero as $k\to\infty$.

IV. ASYMPTOTIC ANALYSIS FOR THE DIATOMIC TODA LATTICE

For diatomic Toda lattice we can obtain an explicit Fredholm solvability condition for the problem (14), (15). Indeed, in this case equations (9) for the slow motion of odd-numbered heavy masses reduce to the equations governing a homogeneous Toda lattice with $a = 1$, $b = 1/2$ in (3) and have an exact solitary wave solution [40]

$$x_{2p-1}(t) = 2\ln\frac{1+\exp[2\kappa(p-1)-t\sqrt{2}\sinh\kappa]}{1+\exp[2\kappa p - t\sqrt{2}\sinh\kappa]} = X(p-c_0t), \quad c_0 = \frac{\sinh(\kappa)}{\sqrt{2}\kappa} \tag{19}$$

Using the second equation in (8), we then obtain the $O(1)$ displacement of the even-numbered light masses:

$$x_{2p}(t) = \ln\frac{1+\exp[2\kappa(p-1)-t\sqrt{2}\sinh\kappa]}{1+\exp[2\kappa(p+1)-t\sqrt{2}\sinh\kappa]}. \tag{20}$$

This yields

$$\Omega_{2p}^2(t) = 2\left\{1+(\sinh^2\kappa)\mathrm{sech}^2\left(\kappa p - \frac{t}{\sqrt{2}}\sinh\kappa\right)\right\} \tag{21}$$

and

$$f_{2p}(t) = -\frac{4\cosh\kappa\sinh^3\kappa\sinh[2\kappa p - t\sqrt{2}\sinh\kappa]}{(\cosh(2\kappa)+\cosh(2\kappa p - t\sqrt{2}\sinh\kappa))^2}. \tag{22}$$

Observe that $f_0(t)$ is an odd function, while $\Omega_0^2(t)$ is even.

The homogeneous equation corresponding to (14) is then a classical problem in quantum mechanics that involves one-dimensional time-independent Schrödinger equation with sech-squared potential of Pöschl-Teller type [45–47] first considered in [48] in the context of wave reflection in an inhomogeneous medium. It can be written as

$$\ddot{y}_0 + \left(\omega^2 + \frac{\nu(\nu+1)\alpha^2}{\cosh^2(\alpha t)}\right)y_0 = 0, \tag{23}$$

where

$$\alpha = \frac{\sinh\kappa}{\sqrt{2}}, \quad \omega = \sqrt{\frac{2}{\varepsilon}}, \quad \nu = \frac{1}{2}\left(-1+\sqrt{1+\frac{16}{\varepsilon}}\right). \tag{24}$$

Substituting $y_0(t) = \psi(\zeta)$, $\zeta = \tanh(\alpha t)$, we obtain the general Legendre equation

$$\frac{d}{d\zeta}\left((1-\zeta^2)\frac{d\psi}{d\zeta}\right) + \left(\nu(\nu+1) + \frac{\omega^2}{\alpha^2(1-\zeta^2)}\right)\psi = 0.$$

This yields two linearly independent solutions of (23) in terms of hypergeometric functions [45],

$$Y_1(t;\varepsilon) = (\cosh(\alpha t))^{\nu+1}{}_2F_1\left(\frac{1}{2}\left[\nu+1+i\frac{\omega}{\alpha}\right], \frac{1}{2}\left[\nu+1-i\frac{\omega}{\alpha}\right], \frac{1}{2}, -\sinh^2(\alpha t)\right) \tag{25}$$

and

$$Y_2(t;\varepsilon) = (\cosh(\alpha t))^{\nu+1}\sinh(\alpha t)_2F_1\left(\frac{1}{2}\left[\nu + i\frac{\omega}{\alpha}\right] + 1, \frac{1}{2}\left[\nu - i\frac{\omega}{\alpha}\right] + 1, \frac{3}{2}, -\sinh^2(\alpha t)\right), \tag{26}$$

which are even and odd, respectively, and have the Wronskian equal to α. We emphasize here that the solutions depend on ε through ν and ω defined in (24) (they also depend on κ through α). Substituting these in (16), we obtain the solution of (14) satisfying $y_0(t) \to 0$ as $t \to -\infty$. Its asymptotic behavior at positive infinity is given by (17) with [45]

$$A = \sqrt{\pi}\left|\frac{\Gamma(i\omega/\alpha)e^{-i\omega\ln 2/\alpha}}{\Gamma(\frac{1}{2}[\nu+2+\frac{i\omega}{\alpha}])\Gamma(\frac{1}{2}[1-\nu+\frac{i\omega}{\alpha}])}\right|, \quad \beta_1 = \arg\frac{\Gamma(i\omega/\alpha)e^{-i\omega\ln 2/\alpha}}{\Gamma(\frac{1}{2}[\nu+1+\frac{i\omega}{\alpha}])\Gamma(-\frac{1}{2}[\nu-\frac{i\omega}{\alpha}])}. \tag{27}$$

and the condition (18) that ensures that $y_0(t) \to 0$ as $t \to \infty$ without oscillations. Meanwhile,

$$Y_2(t;\varepsilon) \sim A\cos(\omega t + \beta_2), \quad t \to \infty, \quad \beta_2 = \arg\frac{\Gamma(i\omega/\alpha)e^{-i\omega\ln 2/\alpha}}{\Gamma(\frac{1}{2}[\nu+2+\frac{i\omega}{\alpha}])\Gamma(\frac{1}{2}[1-\nu+\frac{i\omega}{\alpha}])}. \tag{28}$$

For the diatomic Toda lattice, the function $g(\varepsilon)$ is thus defined by (18), (22) and (26). Letting

$$Y_2(t;\varepsilon) \equiv H(\eta;\varepsilon), \quad \eta = \alpha t, \tag{29}$$

we can rewrite it as

$$g(\varepsilon) = 4\sqrt{2}\cosh(\kappa)\sinh^2(\kappa)\int_0^\infty \Lambda(\eta)H(\eta;\varepsilon)d\eta, \tag{30}$$

where we define

$$\Lambda(\eta) = \frac{\sinh(2\eta)}{[\cosh(2\kappa)+\cosh(2\eta)]^2}. \tag{31}$$

Observe that $\Lambda(\eta) \to 0$ exponentially fast as $\eta \to \infty$, $H(\eta;\varepsilon)$ is bounded for all τ, and for $\varepsilon \in (0,1]$ and $\kappa > 0$, $H(\eta;\varepsilon)$ depends continuously on ε, and both functions depend continuously on κ. This implies that $g(\varepsilon)$ depends continuously on ε and κ in this parameter domain. The integral in (30) can be evaluated numerically for given ε and κ. The calculation simplifies for integer $\nu = N$ in (24), i.e. when $\varepsilon = \epsilon_N \equiv 4/(N(N+1))$ for some integer $N \geq 2$, since in this case $H(\eta;\epsilon_N)$ reduces to an expression in terms of elementary functions [47, 49], and (30) can be computed using contour integration and the residue theorem. As shown in the Appendix, this yields an explicit formula (A7) for $g(\epsilon_N)$.

Fig. 2 shows the typical oscillatory behavior of $g(\varepsilon)$. Since $g(\varepsilon)$ depends continuously on κ, its zeroes ε_k are continuous functions of κ. The first eight such values and the corresponding approximate velocity profiles are shown in Fig. 3. The subscript k in ε_k denotes the number of local maxima in the corresponding velocity function $\dot{y}_0^{(k)}(t)$. Note that the largest of these values,

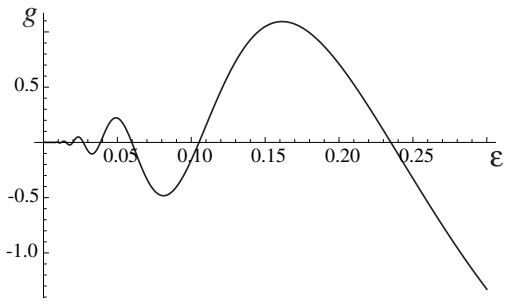

FIG. 2. The oscillatory behavior of $g(\varepsilon)$ defined by (30). Here $\kappa = \text{arcsinh}(2\sqrt{5})$.

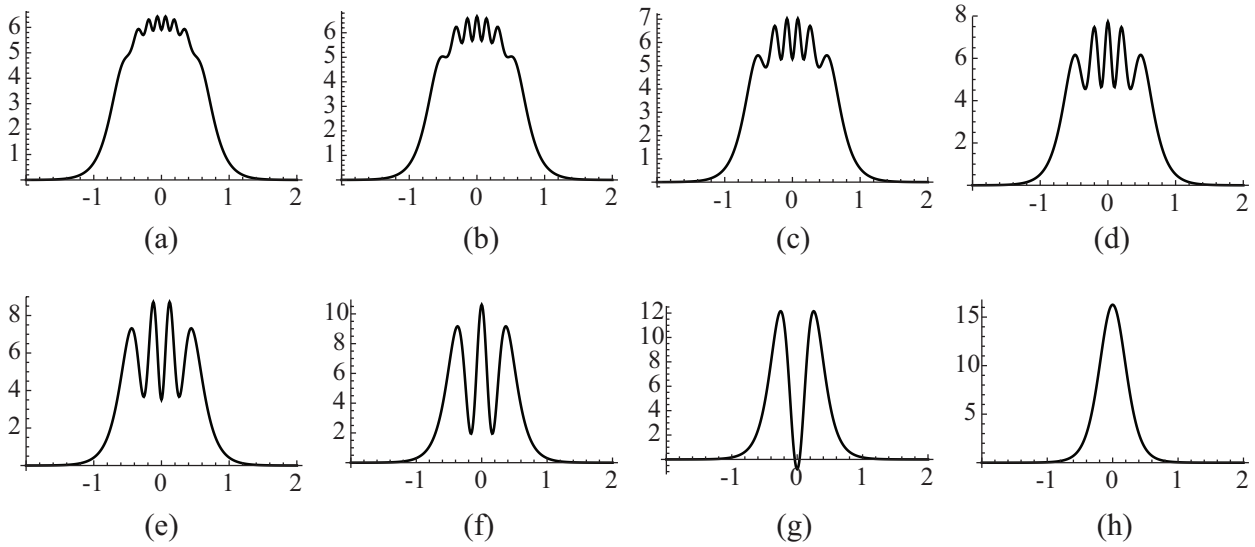

FIG. 3. Approximate velocity profiles $\dot{q}_0(t) \approx \dot{x}_0(t) + \varepsilon \dot{y}_0(t)$ in the diatomic Toda lattice at the special values of ε found by solving (14) subject to (15) (see the text for details): (a) $\varepsilon_8 = 0.0152585$; (b) $\varepsilon_7 = 0.0198633$; (c) $\varepsilon_6 = 0.0269202$; (d) $\varepsilon_5 = 0.0385452$; (e) $\varepsilon_4 = 0.0597712$; (f) $\varepsilon_3 = 0.105242$; (g) $\varepsilon_2 = 0.235084$; (h) $\varepsilon_1 = 0.993342$. Here $\kappa = \text{arcsinh}(2\sqrt{5})$ and $t_0 = 0$.

$\varepsilon_1 \approx 0.993342$, is not small and thus lies beyond the limits of the applicability of the asymptotic analysis. The second largest value, $\varepsilon_2 \approx 0.235084$, is also not small enough for the two time scales to be well separated, so we do not expect it to be a good approximation of the corresponding value in the discrete system (5). But the smaller ε_k values in the asymptotic approximation are expected to be close to the actual ones.

We conjecture that $g(\varepsilon)$ has infinitely many zeroes ε_k in $(0, 1)$ such that $\varepsilon_k \to 0$ as $k \to \infty$. This conjecture is supported by the numerical evaluation of the explicit formula (A7), which suggests that for fixed $\kappa > 0$, $\text{sign}[g(4/(N(N+1))] = -\text{sign}[g(4/((N+2)(N+3))]$ for integer $N \geq 2$. Importantly, the set of ε_k such that $g(\varepsilon_k) = 0$ remains *discrete* at any small but nonzero κ, suggesting that even in the quasicontinuum regime $\kappa \approx 0$ genuine solitary waves can exist only at

certain mass ratios. However, since $g(\varepsilon;\kappa) \to 0$ as $\kappa \to 0$, the amplitude of the trailing oscillations becomes exponentially small at κ near zero [50], which explains why quasicontinuum [17] and KdV [16] approximations of solitary waves for any ε work well in this regime.

V. APPROXIMATE ANTI-RESONANCE CONDITION AT LARGE κ

In the previous section we derived the necessary and sufficient asymptotic condition $g(\varepsilon_n) = 0$, with $g(\varepsilon)$ given by (30), for the anti-resonance values ε_n at which the oscillatory tails in the wake of the primary front vanish in the $O(\varepsilon)$ approximation of the diatomic Toda lattice. However, finding these values generally requires numerical evaluation of (30). In this section we derive a simplified approximate condition valid at large enough κ and $\varepsilon > \varepsilon_{\rm cr}(\kappa)$, where the lower bound $\varepsilon_{\rm cr}$ decreases as κ grows.

To obtain this condition, we first consider the behavior of the functions $\Lambda(\eta)$ and $H(\eta;\varepsilon)$ involved in the integrand of (30) at large κ. Observe that the function $\Lambda(\eta)$ defined in (31) has a single maximum at

$$\eta_{\max} = \operatorname{arccosh}\left[\frac{\sqrt{4 + 2\cosh^2\kappa + \sqrt{2}\sqrt{17 + \cosh(4\kappa)} + 2\sinh^2\kappa}}{2\sqrt{2}}\right] \approx \kappa, \quad \kappa \gg 1$$

Moreover, for large κ this function has an exponentially localized bell-shaped form with an approximate even symmetry about its maximum:

$$\Lambda(\eta_{\max} - \chi) \approx \Lambda(\eta_{\max} + \chi), \quad \kappa \gg 1, \tag{32}$$

because

$$\Lambda(\eta_{\max} + \chi) \approx \frac{\exp(-2\kappa)}{2\cosh^2\chi}, \quad \kappa \gg 1.$$

For $\kappa = 10$ this is illustrated by the dashed curve in Fig. 4. The half-width $\chi_{\rm w}$ of this pulse, defined by

$$\Lambda(\eta_{\max} + \chi_{\rm w}) = 0.01\Lambda(\eta_{\max}),$$

approaches a constant value $\chi_{\rm w} \approx 2.993$ at $\kappa \gg 1$. Meanwhile, the function H defined in (29) (the solid curve in Fig. 4) has fast oscillations for small enough $\eta > 0$, while for larger η there are slower oscillations that are asymptotically described by

$$H \approx A(\varepsilon,\kappa)\cos\left(\frac{2\eta}{\sqrt{\varepsilon}\sinh(\kappa)} + \beta_2(\varepsilon,\kappa)\right), \quad \eta \gg 1 \tag{33}$$

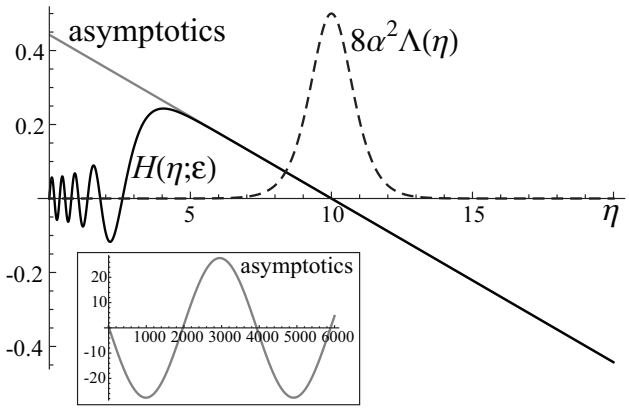

FIG. 4. The functions $H(\eta;\varepsilon)$ (solid curve), its asymptotic approximation (33) (gray curve) and $8\alpha^2\Lambda(\eta)$ (dashed curve) at $\kappa = 10$. Inset: the asymptotic approximation over a larger interval. Here $\varepsilon = 0.01285078$ and (34) holds.

(gray curve in Fig. 4), where we recall that A, defined in (27), and β_2, given in (28), are functions of ε and κ through α, ω and ν defined in (24). In what follows, we fix a small threshold $\delta > 0$ measuring the accuracy of the approximation (33). The asymptotic approximation then becomes valid (i.e. its absolute error is less than δ) for $\eta > \eta_{\rm a}(\kappa,\varepsilon)$, where $\eta_{\rm a}$ increases with κ at fixed ε, approaching a value that depends only on ε for large enough κ, and decreases as ε grows at fixed κ. This implies that there exist $\eta_{\rm cr}$ and $\varepsilon_{\rm cr}$, depending on κ, such that for given κ the approximation error is less than δ for $\eta > \eta_{\rm cr}$ and $\varepsilon > \varepsilon_{\rm cr}$. Here $\varepsilon_{\rm cr}$ decreases as κ is increased.

Suppose now that κ is large enough so that (i) the approximate even symmetry (32) of $\Lambda(\eta)$ holds and (ii) the pulse of $\Lambda(\eta)$ is localized inside the region where the asymptotic approximation (33) accurately describes $H(\eta;\varepsilon)$ for $\varepsilon > \varepsilon_{\rm cr}(\kappa)$, i.e. $\eta_{\rm max} - \chi_{\rm w} \geq \eta_{\rm cr}(\kappa)$. Both conditions hold, for example, in Fig. 4, where $\kappa = 10$, $\eta_{\rm max} - \chi_{\rm w} \approx 7.007$, and the absolute error of the asymptotic approximation of H is less than $\delta = 2.3 \times 10^{-5}$ for $\eta > \eta_{\rm cr} = 7$. Let η_0 be such that $\eta_0 > \eta_{\rm cr}(\kappa)$ and $H(\eta_0) = 0$. The second condition then ensures that H has an approximate odd symmetry about η_0 since the approximation (33) has an exact odd symmetry about its zeroes. Together with the approximate even symmetry of Λ about $\eta = \eta_{\rm max}(\kappa)$, this implies that the integral (30) will be approximately zero if $\eta_0 = \eta_{\rm max}$, i.e. the peak of Λ occurs *exactly* at the point where H vanishes:

$$H(\eta_{\rm max}(\kappa);\varepsilon) = 0. \tag{34}$$

Physically, this corresponds to the largest magnitude of the acceleration of the center of mass between the two heavy masses occuring precisely at the moment when the free fast oscillation of the light mass in between goes through zero. Using the asymptotic approximation (33), the

condition (34) can be further simplified to yield

$$\frac{2\eta_{\max}(\kappa)}{\sqrt{\varepsilon}\sinh(\kappa)} + \beta_2(\varepsilon,\kappa) = \frac{\pi}{2}\mathrm{sign}[\beta_2(\varepsilon,\kappa)], \tag{35}$$

where the sign in front of $\pi/2$ in the right hand side is determined by the (nonzero) phase $\beta_2(\varepsilon,\kappa)$ of the oscillations.

We checked (34) and (35) for $\kappa = 10$ and verified that both yield the values of ε_n that are in an excellent agreement, up to the relative error of $O(10^{-8})$, with the values obtained using numerical approximation of (30) (while the relative error of the roots of (35) approximating the zeroes of (34) is $O(10^{-9})$ for the smaller computed values). In all three cases, the first several values are $\varepsilon_2 = 0.3109212$, $\varepsilon_3 = 0.1272799$, $\varepsilon_4 = 0.06894426$, $\varepsilon_5 = 0.04318148$, $\varepsilon_6 = 0.02957127$, $\varepsilon_7 = 0.02151489$, $\varepsilon_8 = 0.01635427$, $\varepsilon_9 = 0.01285078$. As expected, the approximation error is smaller for larger ε_n. At $\kappa = 5$ the asymptotic approximation is not accurate over the entire interval where $\Lambda(\eta)$ is localized for smaller ε. As a result, the relative errors of the approximations are larger but still fairly small, up to $O(10^{-3})$ for the solutions of (34) approximating the first few roots of (30), given in this case by $\varepsilon_2 = 0.2824200$, $\varepsilon_3 = 0.1184396$, $\varepsilon_4 = 0.06497014$, $\varepsilon_5 = 0.04102020$, $\varepsilon_6 = 0.02825095$, $\varepsilon_7 = 0.02064249$, $\varepsilon_8 = 0.01574431$, $\varepsilon_9 = 0.01002809$, and up to $O(10^{-4})$ for the roots of (35) approximating the zeroes of (34).

VI. NUMERICAL RESULTS

To find the special values of ε for the discrete system, we ran the numerical simulations of (5) with $\phi'(r) = 1 - e^{-r}$ employing the symplectic Candy-Rozmus algorithm. The solution of (8) was used as the initial condition. Recall that this solution is given by (19) and (20) for heavy odd-numbered and light even-numbered masses, respectively, and depends on the parameter κ that determines the amplitude and velocity of the wave. For given κ we sought the values of ε at which the energy stored at a fixed site $n = n_0$ was close to zero at a time instant $t = t_a$ after the pulse has left the site. For example, at $\kappa = \mathrm{arcsinh}(2\sqrt{5})$ we used $n_0 = 200$ and $t_a = 40$. The results for this value of κ are compared in Table I with the corresponding values obtained using the asymptotic analysis. As expected, the approximation works very well for smaller values of ε_k, but as ε_k becomes larger the predicted values yield progressively poorer approximation. In particular, the largest value, $\varepsilon_2 \approx 0.319089$, is not very close to the value 0.235084 obtained from the asymptotic analysis. At this value the velocity of the light mass has two maxima. There appears to be no value $\varepsilon_1 < 1$ with a single maximum (although of course such solutions, Toda solitons, exist in the monatomic case

k	ε_k from (18)	ε_k from (5)
2	0.235084	0.319089
3	0.105242	0.116993
4	0.0597712	0.0633882
5	0.0385452	0.0402105
6	0.0269202	0.0275323
7	0.0198633	0.0201695
8	0.0152585	0.0154320

TABLE I. The values of ε obtained from the Fredholm condition (18) and from the numerical solution of (5) with $\phi'(r) = 1 - e^{-r}$ and initial conditions determined from (19), (20) at $\kappa = \text{arcsinh}(2\sqrt{5})$.

$\varepsilon = 1$); as discussed above, the spurious value of ε_1 obtained from the asymptotic analysis, lies well beyond the validity domain of the multiscale expansion and thus should be discarded.

Fig. 5 and Fig. 6 show the corresponding velocity profiles for even-numbered light masses (solid curves) and odd-numbered heavy masses (dotted curves). Note that the light-mass velocity profiles are similar to the ones shown in Fig. 3, with the number of local maxima increasing as ε_k becomes smaller. Observe also that the velocity of the solitary wave at $\varepsilon = \varepsilon_k$ increases with k and approaches the speed $2c_0 = \sinh(\kappa)\sqrt{2}/\kappa$ of the $\varepsilon = 0$ chain of only heavy masses described by (9).

Homoclinic orbits for light (solid curves) and heavy (dotted curves) masses corresponding to the solutions at $\varepsilon = \varepsilon_8$ and $\varepsilon = \varepsilon_4$ are shown in Fig. 7. One can see that the orbits corresponding to the light masses exhibit oscillations and, at larger ε_k, small loops.

The values of ε_k change slightly as κ is varied, and their dependence on κ is non-monotone, as can be seen in Fig. 8 where the velocity profiles at ε_2 for different κ are shown. Note that while ε_2 depends only only weakly on κ, the solitary wave profiles change significantly as κ is varied. Their amplitude and the amplitude of oscillations of the light mass grow with κ, as does the propagation speed.

VII. CLOSING REMARKS

In this work we have focused on the mechanism of formation of the isolated localized wave structures existing in the diatomic FPU model of the general type. We demonstrated numerically that there is a sequence of special mass ratios at which the diatomic Toda lattice supports formation of genuine solitary waves. Further, the asymptotic analysis based on the singular multiscale expansion effectively reduces the complex structure of the diatomic FPU chain to the externally driven

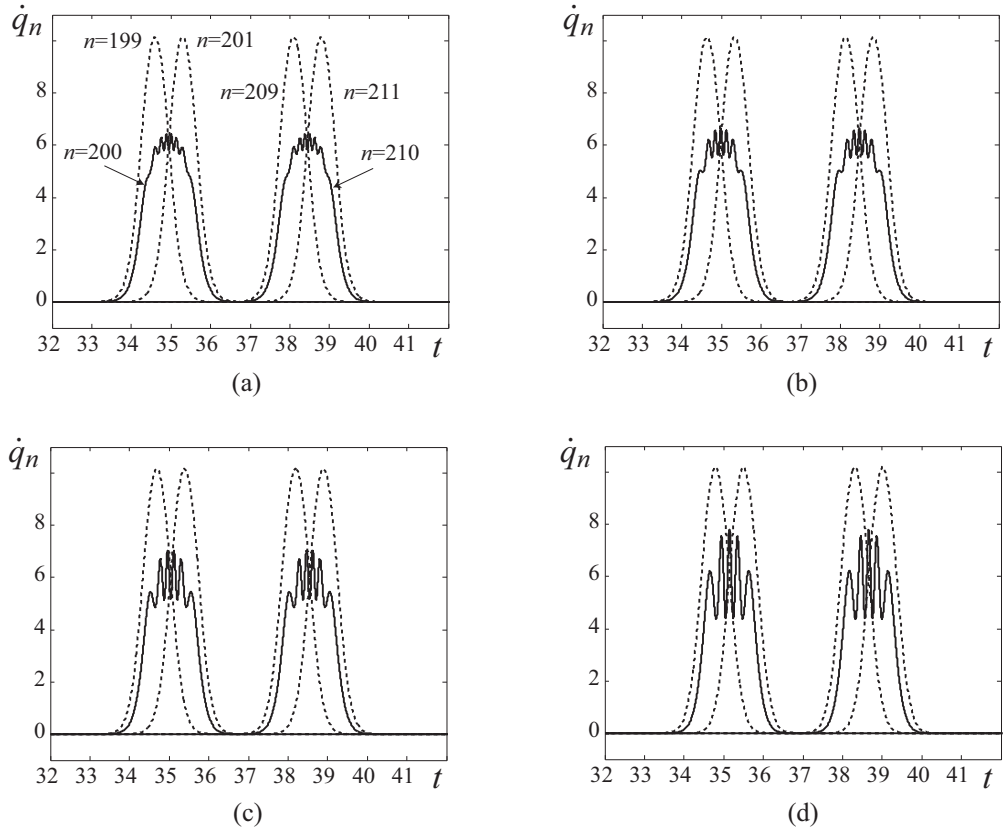

FIG. 5. Velocity profiles $\dot{q}_n(t)$ at four smaller special values of ε for light (solid curves) and heavy (dotted curves) masses at $n = 199$, 200, 201 and $n = 209$, 210, 211: (a) $\varepsilon_8 = 0.0154320$; (b) $\varepsilon_7 = 0.0201695$; (c) $\varepsilon_6 = 0.0275323$; (d) $\varepsilon_5 = 0.0402105$. Initial conditions were determined from (19), (20) with $\kappa = \operatorname{arcsinh}(2\sqrt{5})$.

linear oscillator with time-varying frequency. Using the derived reduced-order approximation, we formulated the anti-resonance Fredholm orthogonality condition on the mass ratio supporting the formation of solitary waves in the general class of the diatomic FPU models and conjectured the existence of a countable infinite sequence of such ratios. To illustrate this result, we considered the diatomic Toda lattice in the limit of high mass mismatch. We showed that in this case the derived asymptotic equations have exact solutions, reducing the Fredholm orthogonality condition to orthogonality of two explicitly known functions. This is in contrast to the previously considered case of granular crystals [24], where the authors had to use the WKB approximation of the fast dynamics and an exponential Padé approximation [51] of the slow heavy-mass wave in order to obtain the results. Meanwhile, in the diatomic Toda setting, the problem involves explicit solutions of the Schrödinger equation with Pöshl-Teller type potential and the exact solitary wave solutions of the monatomic Toda lattice. Using asymptotic behavior of the former, we obtained a simplified condition that works extremely well for large enough values of κ and ε and has a nice physical in-

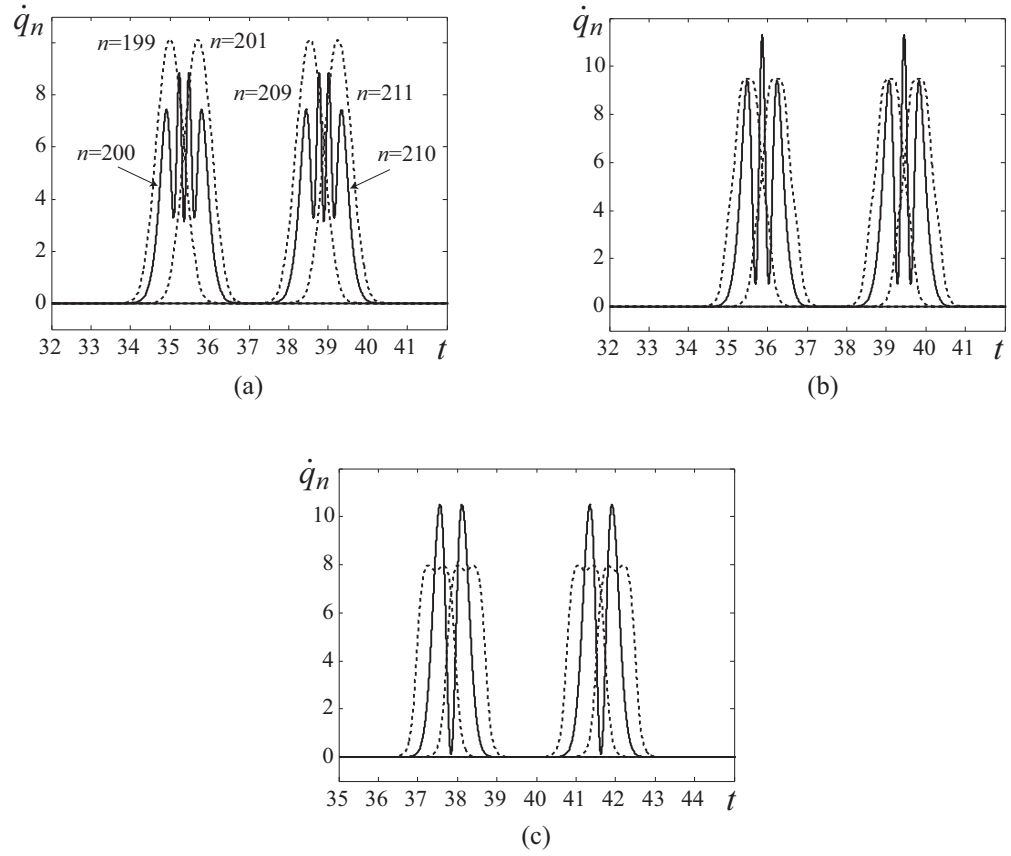

FIG. 6. Velocity profiles $\dot{q}_n(t)$ at three larger special values of ε for light (solid curves) and heavy (dotted curves) masses at $n = 199$, 200, 201 and $n = 209$, 210, 211: (a) $\varepsilon_4 = 0.0633882$; (b) $\varepsilon_3 = 0.116993$; (c) $\varepsilon_2 = 0.319089$. Initial conditions were determined from (19), (20) with $\kappa = \text{arcsinh}(2\sqrt{5})$.

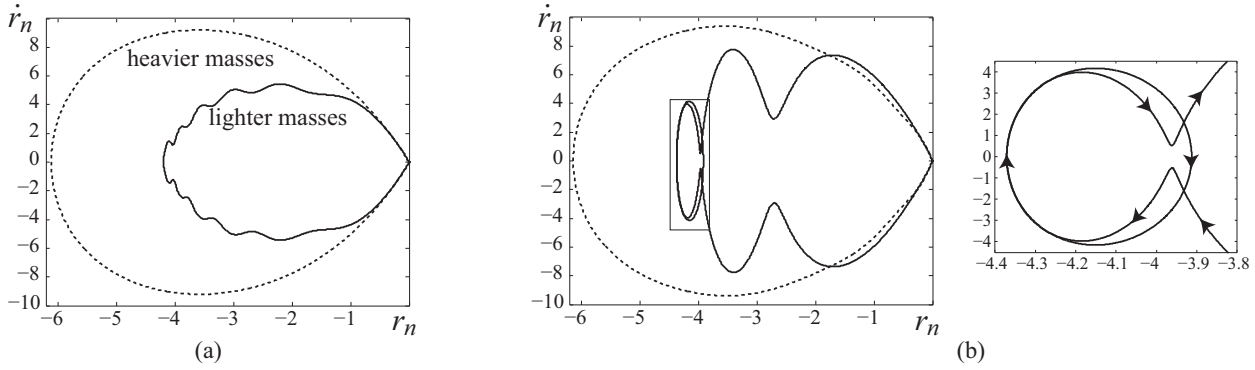

FIG. 7. Homoclinic orbits for light (solid curves) and heavy (dotted curves) masses corresponding to the solutions shown in Fig. 5 and Fig. 6 at (a) $\varepsilon = \varepsilon_8 = 0.0154320$ and (b) $\varepsilon = \varepsilon_4 = 0.0633882$. Here $r_n = q_{n+2} - q_n$ is the relative displacement between the neighboring heavy (odd n) or light (even n) masses, and $\dot{r}_n$ is the relative velocity. The smaller plot on the right in (b) shows the enlarged view of the region inside the rectangle in the larger plot in (b), with the arrows indicating the direction of increasing time.

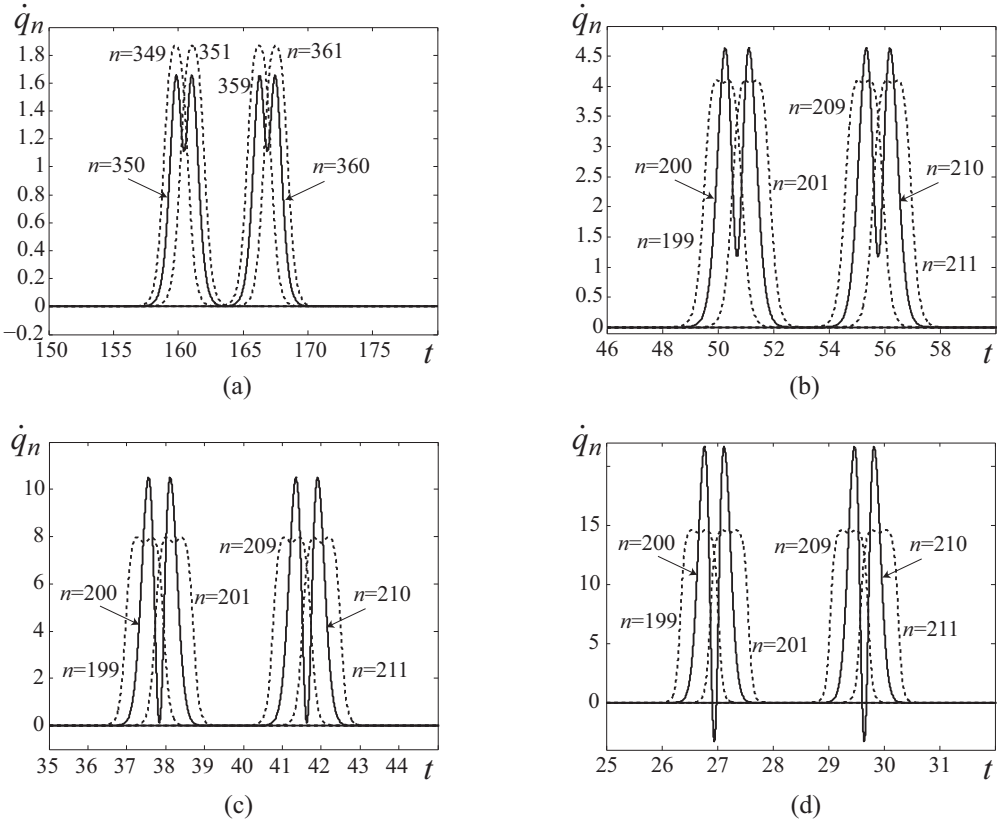

FIG. 8. Velocity profiles $\dot{q}_n(t)$ at ε_2 computed for different values of κ for light (solid curves) and heavy (dotted curves) masses: (a) $\varepsilon_2 = 0.314544$, $\kappa = 1.10164$; (b) $\varepsilon_2 = 0.319694$, $\kappa = 1.65246$; (c) $\varepsilon_2 = 0.319089$, $\kappa = 2.20329$; (d) $\varepsilon_2 = 0.313788$, $\kappa = 2.75411$. Initial conditions were determined from (19), (20) with the corresponding κ.

terpretation. The obtained analytical predictions of the discrete set of values of the anti-resonance mass ratios are in an excellent agreement with the values obtained from the numerical simulations of the full diatomic Toda lattice at small enough ε.

Existence of isolated solitary wave solutions in a diatomic FPU lattice implies that one can tune the mass ratio to be close to one of the anti-resonance values and ensure that an impact-initiated wave transfers energy through the chain with minimal loss. One can also tune the mass ratio to a near-resonance value for maximal energy loss that could be used for impact mitigation [52]. For strongly nonlinear granular chains, the existence of such resonance and anti-resonance values of mass ratios was recently experimentally verified in [53]. More generally, the existence result can be extended to plane solitary waves in two-dimensional diatomic lattices when the problem can be reduced to an effective one-dimensional FPU chain that has isolated solitary wave solutions. For two-dimensional diatomic granular crystals under planar impact, existence of a discrete set of mass ratios in the high mismatch asymptotic limit was recently shown in [54] by extending the

results in [24]. Another natural extension of this work is to consider dimer lattices with each pair of heavy masses separating $N \geq 2$ light ones. Granular chains of this type were studied in [42], where the asymptotic analysis suggests existence of a countable infinity of isolated solitary waves in the case $N = 2$, while for $N > 2$ the authors claim non-existence of such solutions. It would be interesting to check if the same assertions hold for the dimer as well as the trimer Toda lattices. Another important problem to be considered in the future is the analysis of the similar isolated wave structures in the diatomic and triatomic FPU models incorporating long range interactions.

In this work we were able to take full advantage of the integrability of the monatomic Toda lattice to obtain an explicit orthogonality condition in the non-integrable diatomic case. In the general FPU case, the Fredholm orthogonality condition (18) requires the knowledge of $f_0(t)$ and $Y_2(t)$, which are not typically explicitly available. Using a good approximation of the slow-time solitary pulse that yields $f_0(t)$ and applying the WKB approach to find $Y_2(t)$ may prove sufficient in such cases, as demonstrated in [24]. Nevertheless, proving the existence of a countable infinity of isolated solitary waves in a diatomic FPU lattice, conjectured in this work in the small-ε asymptotic limit under fairly general assumptions, remains an open problem. Even in the diatomic Toda case, the complex nature of the function (30) prevented us from showing that it has infinitely many roots, although we have plenty of numerical evidence supporting this claim. An even more challenging question is showing this result beyond the asymptotic approximation, which would definitively establish existence of such waves even at mass ratios that are not very small, when separation of time scales no longer takes place.

ACKNOWLEDGMENTS

The authors thank Aaron Hoffman and Dmitry Pelinovsky for insightful discussions. Support by the U.S. National Science Foundation through the grants DMS-1506904 (A.V.), DMS-1105635 and DMS-1511488 (J.D.W.) is gratefully acknowledged. The second author (Y.S.) thanks Israeli Science Foundation (grant 484/12) and Pazi (grant 263/15) for financial support.

Appendix A: Evaluation of g for integer ν

Let $N \geq 2$ be an integer and let

$$\epsilon_N = \frac{4}{N(N+1)}, \quad \mu_N = \frac{\sqrt{N(N+1)}}{\sinh(\kappa)}. \tag{A1}$$

Note that $\varepsilon = \epsilon_N$ corresponds to $\nu = N$ and $\omega/\alpha = \mu_N$ in (24). Then $H(\eta;\epsilon_N)$ defined in (29) is an odd function of η satisfying

$$\frac{d^2H}{d\eta^2} + \left(\mu_N^2 + N(N+1)\mathrm{sech}^2(\eta)\right) H = 0. \tag{A2}$$

and

$$H(0;\epsilon_N) = 1. \tag{A3}$$

Equation (A2) has a non-odd solution in the form [49]

$$\Psi_N(\eta) = \frac{e^{i\mu_N\eta}}{(1+e^{-2\eta})^N} \sum_{m=0}^{N} C_m^N \binom{N}{m} e^{-2m\eta}, \tag{A4}$$

with

$$C_m^N = \prod_{j=1}^{m} \frac{i\mu_N + N + 1 - j}{i\mu_N - j}, \quad m \geq 1$$

and $C_0^N = 1$. One can show that $\Psi_N'(0) \neq 0$. Note that since $\mathrm{sech}^2(\eta)$ is even, $\Psi_N(-\eta)$ is also a solution of (A2). The odd solution of (A2) satisfying (A3) is then given by

$$H(\eta;\epsilon_N) = \frac{1}{2\Psi_N'(0)} \left[\Psi_N(\eta) - \Psi_N(-\eta)\right].$$

Using this and (30), we obtain

$$g(\epsilon_N) = \frac{2\sqrt{2}\cosh(\kappa)\sinh^2(\kappa)}{\Psi_N'(0)} \int_{-\infty}^{\infty} \Lambda(\eta)\Psi_N(\eta)d\eta. \tag{A5}$$

The integral in (A5) can be evaluated using contour integration in the complex plane $\mathbb{C}$. Observe that at $\kappa > 0$ the well known properties of complex exponentials imply that

(a) $\Lambda(\eta + i\pi) = \Lambda(\eta)$ for all $\eta \in \mathbb{C}$.

(b) The singularities of $\Lambda(\eta)$ are located at $\eta = \eta_{\pm 1} + in\pi$, where $n \in \mathbb{Z}$ and $\eta_{\pm 1} = \pm\kappa + \frac{i\pi}{2}$. All such singularities are poles of order 2.

(c) $\Lambda(\eta)$ has simple zeros at $\eta = \eta_0 + in\pi$, where $n \in \mathbb{Z}$ and $\eta_0 = \frac{i\pi}{2}$.

(d) $\Psi_N(\eta + i\pi) = e^{-\mu_N\pi}\Psi_N(\eta + i\pi)$ for all $\eta \in \mathbb{C}$.

(e) The singularities of $\Psi_N(\eta)$ are are located at $\eta = \eta_0 + in\pi$, where $n \in \mathbb{Z}$. All such singularities are poles of order N.

Thus we see that the integrand $\Lambda(\eta)\Psi_N(\tau)$ in (A5) has a pole of order $N-1$ at $\eta=\eta_0$ defined in (c) and poles of order 2 at $\eta_{\pm 1}$ defined in (b). Moreover, one can show that there exists a constant $\rho>0$ such that

$$|\Lambda(\pm R+i\gamma)\Psi_N(\pm R+i\gamma)|\leq \rho e^{-\rho R} \tag{A6}$$

when $R>2\kappa$ and $\gamma\in[0,\pi]$.

Now let $R>2\kappa$. By the residue theorem,

$$\int_{C_R}\Lambda(\eta)\Psi_N(\eta)d\eta = 2\pi i\sum_{j=-1}^{1}\mathrm{Res}(\Lambda\Psi_N,\eta_j),$$

where C_R is the closed positively oriented rectangular curve in $\mathbb{C}$ with bottom side given by the interval $[-R,R]$ along the real line, right and left sides given by $\tau=\pm R+i\gamma$, $\gamma\in[0,\pi]$ and top side given by the horizontal line segment from $-R+i\pi$ to $R+i\pi$. In the limit $R\to\infty$, the estimate (A6) implies that the integrals over the left and right sides of C_R vanish. The relation (d) implies that the integral over the top side is $-e^{-\mu_N\pi}$ times the integral over the bottom side of the rectangle. Finally, as $R\to\infty$, the integral on the bottom side converges to the desired integral in (A5). Thus we obtain

$$\int_{-\infty}^{\infty}\Lambda(\eta)\Psi_N(\eta)d\eta = (1-e^{-\mu_N\pi})^{-1}2\pi i\sum_{j=-1}^{1}\mathrm{Res}(\Lambda\Psi_N,\eta_j).$$

Together with (A5), this yields the following explicit expression for $g(\epsilon_N)$:

$$g(\epsilon_N)=\frac{4\sqrt{2}\pi i\cosh(\kappa)\sinh^2(\kappa)}{(1-e^{-\mu_N\pi})\Psi_N'(0)}\sum_{j=-1}^{1}\mathrm{Res}(\Lambda\Psi_N,\eta_j). \tag{A7}$$

---

[1] A. Scott, *Nonlinear Science: Emergence and Dynamics of Coherent Structures* (Oxford University Press, 2003).

[2] T. Dauxois and M. Peyrard, *Physics of Solitons* (Cambridge University Press, 2006).

[3] M. Remoissenet, *Waves Called Solitons: Concepts and Experiments* (Springer, 2003).

[4] E. Fermi, J. Pasta, and S. Ulam, *Studies of nonlinear problems*, Tech. Rep. LA-1940 (Los Alamos Scientific Laboratory, 1955).

[5] N. J. Zabusky and M. D. Kruskal, Phys. Rev. Lett. **15**, 240 (1965).

[6] D. K. Campbell, P. Rosenau, and G. M. Zaslavsky, Chaos **15** (2005).

[7] G. Friesecke and J. A. D. Wattis, Commun. Math. Phys. **161**, 391 (1994).

[8] F. Mokross and H. Buttner, J. Phys. C **16**, 4539 (1983).

[9] H. Bilz, H. Büttner, A. Bussmann-Holder, W. Kress, and U. Schröder, Phys. Rev. Lett. **48**, 264 (1982).

[10] V. Y. Antonchenko, A. S. Davydov, and A. V. Zolotariuk, Phys. Status Solidi (b) **115**, 631 (1983).

[11] M. J. Rice and E. J. Mele, Phys. Rev. Lett. **49**, 1455 (1982).

[12] S. Pnevmatikos, M. Remoissenet, and N. Flytzanis, J. Phys. C **16**, L305 (1983).

[13] S. Pnevmatikos, N. Flytzanis, and M. Remoissenet, Phys. Rev. B **33**, 2308 (1986).

[14] A. Mielke, Arch. Ration. Mech. Anal. **181**, 401 (2006).

[15] M. Chirilus-Bruckner, C. Chong, O. Prill, and G. Schneider, Discrete Contin. Dyn. Syst. Ser. S **5**, 879 (2012).

[16] J. Gaison, S. Moskow, J. Wright, and Q. Zhang, Mult. Model. Simul. **12**, 953 (2014).

[17] M. A. Collins, Phys. Rev. A **31**, 1754 (1985).

[18] G. Huang, Phys. Rev. B **51**, 12347 (1995).

[19] J. A. D. Wattis, Phys. Lett. A **284**, 16 (2001).

[20] R. B. Tew and J. A. D. Wattis, J. Phys. A **34**, 7163 (2001).

[21] M. Hörnquist and R. Riklund, J. Phys. Soc. Japan **65**, 2872 (1996).

[22] Y. Okada, S. Watanabe, and H. Tanaca, J. Phys. Soc. Japan **59**, 2647 (1990).

[23] Y. Tabata, J. Phys. Soc. Japan **65**, 3689 (1996).

[24] K. R. Jayaprakash, Y. Starosvetsky, and A. F. Vakakis, Phys. Rev. E **83**, 036606 (2011).

[25] J. Fujioka and A. Espinosa, J. Phys. Soc. Japan **66**, 2601 (1997).

[26] A. R. Champneys, B. A. Malomed, and M. J. Friedman, Phys. Rev. Lett. **80**, 4169 (1998).

[27] A. R. Champneys and B. A. Malomed, J. Phys. A **32**, L547 (1999).

[28] J. Yang, B. A. Malomed, and D. J. Kaup, Phys. Rev. Lett. **83**, 1958 (1999).

[29] J. Yang, B. A. Malomed, and D. J. Kaup, Math. Comp. Simul. **56**, 585 (2001).

[30] A. Espinosa-Cerón, J. Fujioka, and A. Gómez-Rodríguez, Phys. Scripta **67**, 314 (2003).

[31] A. R. Champneys and B. A. Malomed, Phys. Rev. E **61**, 886 (2000).

[32] W. C. K. Mak, B. A. Malomed, and P. L. Chu, Phys. Rev. E **58**, 6708 (1998).

[33] R. F. Rodríguez, J. A. Reyes, A. Espinosa-Cerón, J. Fujioka, and B. A. Malomed, Phys. Rev. E **68** (2003).

[34] J. Yang, Stud. Appl. Math. **106**, 337 (2001).

[35] S. González-Pérez-Sandi, J. Fujioka, and B. A. Malomed, Phys. D. **197**, 86 (2004).

[36] D. E. Pelinovsky and J. Yang, Proc. R. Soc. Lond. A **458**, 1469 (2002).

[37] T. Wagenknecht and A. R. Champneys, Phys. D **177**, 50 (2003).

[38] D. J. Kaup and B. A. Malomed, Physica D **184**, 153 (2003).

[39] G. Alfimov, E. Medvedeva, and D. Pelinovsky, Phys. Rev. Lett. **112** (2014).

[40] M. Toda, *Theory of nonlinear lattices* (Springer, Berlin, 1981).

[41] S. Ishiwata, S. Matsutani, and Y. Nishi, Phys. Lett. A **231**, 208 (1997).

[42] K. R. Jayaprakash, Y. Starosvetsky, and A. F. Vakakis, J. Appl. Phys. **112**, 1 (2012).

[43] V. Nesterenko, *Dynamics of Heteregeneous Materials* (Springer, 2001).

[44] M. A. Porter, C. Daraio, E. B. Herbold, I. Szelengowicz, and P. G. Kevrekidis, Phys. Rev. E **77**, 1 (2008).

[45] S. Flügge, *Practical Quantum Mechanics*, Vol. 1 (Springer-Verlag, 1971).

[46] L. D. Landau and E. M. Lifshits, *Quantum Mechanics* (Pergamon Press, 1965).

[47] J. Lekner, Amer. J. Phys. **75**, 1151 (2007).

[48] P. S. Epstein, Proc. Nat. Acad. Sci. USA **16**, 627 (1930).

[49] J. F. Van Diejen and A. N. Kirillov, Adv. Math. **149**, 61 (2000).

[50] T. E. Faver and J. D. Wright, arXiv preprint arXiv:1511.00942 (2015).

[51] S. Sen, J. Hong, J. Bang, E. Avalos, and R. Doney, Phys. Rep. **462**, 21 (2008).

[52] K. R. Jayaprakash, Y. Starosvetsky, A. F. Vakakis, and O. V. Gendelman, J. Nonlin. Sci. **23**, 363 (2013).

[53] R. Potekin, K. R. Jayaprakash, D. M. McFarland, K. Remick, L. A. Bergman, and A. F. Vakakis, Exper. Mech. **53**, 861 (2013).

[54] M. Manjunath, A. P. Awasthi, and P. H. Geubelle, Phys. Rev. E **90**, 032209 (2014).